

Journal Pre-proof

IgG glycosylation associates with risk of progression from latent to active tuberculosis
Running title: IgG glycosylation and active tuberculosis risk

Julie G Burel, Wenjun Wang, Manfred Wuhrer, Martin Dedicoat, Thomas E Fletcher, Adam F Cunningham, Matthew K O'Shea



PII: S0163-4453(24)00033-1

DOI: <https://doi.org/10.1016/j.jinf.2024.01.014>

Reference: YJINF6115

To appear in: *Journal of Infection*

Accepted date: 28 January 2024

Please cite this article as: Julie G Burel, Wenjun Wang, Manfred Wuhrer, Martin Dedicoat, Thomas E Fletcher, Adam F Cunningham and Matthew K O'Shea, IgG glycosylation associates with risk of progression from latent to active tuberculosis
Running title: IgG glycosylation and active tuberculosis risk, *Journal of Infection*, (2024) doi:<https://doi.org/10.1016/j.jinf.2024.01.014>

This is a PDF file of an article that has undergone enhancements after acceptance, such as the addition of a cover page and metadata, and formatting for readability, but it is not yet the definitive version of record. This version will undergo additional copyediting, typesetting and review before it is published in its final form, but we are providing this version to give early visibility of the article. Please note that, during the production process, errors may be discovered which could affect the content, and all legal disclaimers that apply to the journal pertain.

© 2024 Published by Elsevier.

IgG glycosylation associates with risk of progression from latent to active tuberculosis

Running title: IgG glycosylation and active tuberculosis risk

Julie G Burel¹, Wenjun Wang², Manfred Wuhrer², Martin Dedicoat³, Thomas E Fletcher^{4,5}, Adam F Cunningham⁶, Matthew K O'Shea^{3,5,6,*}

¹ Center for Infectious Disease and Vaccine Research, La Jolla Institute for Immunology, La Jolla, CA, USA

² Center for Proteomics and Metabolomics, Leiden University Medical Center, Leiden, the Netherlands

³ Department of Infection, University Hospitals Birmingham NHS Foundation Trust, Birmingham, UK

⁴ Department of Clinical Sciences, Liverpool School of Tropical Medicine, Liverpool, UK

⁵ Academic Department of Military Medicine, Royal Centre for Defence Medicine, Birmingham, UK

⁶ Institute of Immunology and Immunotherapy, University of Birmingham, Birmingham, UK

* Correspondence to:

Dr Matthew K. O'Shea, Institute of Immunology and Immunotherapy, University of Birmingham, Birmingham, B15 2TT, UK, M.K.OSHEA@bham.ac.uk, +44 (0)121 414 4068

Abstract

Objectives: Glycosylation motifs shape antibody structure, stability and antigen affinity and play an important role in antibody localization and function. Serum IgG glycosylation profiles are

significantly altered in infectious diseases, including tuberculosis (TB), but have not been studied in the context of progression from latent to active TB.

Methods: We performed a longitudinal study of paired bulk IgG glycosylation and transcriptomic profiling in blood from individuals with active TB (ATB) or latent TB infection (LTBI) before and after treatment.

Results: We identified that a combination of two IgG1 glycosylation traits were sufficient to distinguish ATB from LTBI with high specificity and sensitivity, prior to, and after treatment. Importantly, these two features positively correlated with previously defined cellular and RNA signatures of ATB risk in LTBI, namely monocyte to lymphocyte ratio and the expression of interferon (IFN)-associated gene signature of progression (IFN-risk signature) in blood prior to treatment. Additional glycosylation features at higher prevalence in LTBI individuals with high expression of the IFN-risk signature prior to treatment included fucosylation on IgG1, IgG2 and IgG3.

Conclusions: Together, our results demonstrate that bulk IgG glycosylation features could be useful in stratifying the risk of LTBI reactivation and progression to ATB.

Keywords

Tuberculosis; IgG glycosylation; blood biomarkers; transcriptomics

Introduction

Glycosylation is a post-translational modification naturally occurring on the majority of human proteins, including immunoglobulins (Ig). IgG is the most abundant Ig class in human blood and plays a central role in protective immunity against infectious diseases. On IgG, glycosylation occurs predominantly at one specific residue on the fragment crystallizable (Fc) domain (Asparagine 297), commonly referred to as Fc N-glycosylation (1). Since the Fc region interacts

with various key components of the immune system such as Ig receptors and complement molecules (1), Fc N-glycosylation impacts not only the structure and stability of IgG antibodies, but also their effector functions (2, 3).

IgG Fc N-glycosylation profiles can vary with age and inflammation, for example, galactosylation of IgG is decreased in the elderly (4). Low levels of sialylation and galactosylation, combined with high levels of fucosylation, are associated with auto-immunity, inflammation, and poor metabolic health (5, 6). The absence of fucosylation on IgG Fc N-glycans results in increased affinity for Fc gamma receptor III and enhanced antibody-mediated cellular cytotoxicity (ADCC) (7). More generally, low levels of IgG1 Fc N-galactosylation may serve as a predictor of immune cell activation (8). Additionally, IgG N-glycosylation can be reshaped within an individual in response to changes in the environment, for instance vaccine administration (9), or the presence of a pathogen, such as *Mycobacterium tuberculosis* (*Mtb*) infection (10-13).

Following infection with *Mtb*, most individuals control the bacilli through innate and adaptive immune mechanisms and remain in an asymptomatic state of latent tuberculosis infection (LTBI) (14). In some cases, *Mtb* escapes containment which leads to the development of symptomatic disease, termed active TB (ATB) (15). The World Health Organization guidelines for managing LTBI estimates that the average risk of individuals with LTBI progressing to ATB is 5-10% over their lifetime, and is increased with immunodeficiency (16). A current challenge for global TB control strategies is to identify individuals within the LTBI pool at greatest risk of developing ATB (i.e., LTBI progressors).

There are no diagnostic tests at present that can formally identify LTBI progressors, although multiple groups have identified blood leukocyte and gene expression profiles that are associated with progression from LTBI to ATB. The monocyte to lymphocyte ratio has been repeatedly

proposed as a biomarker for diagnosis, but also prognosis of ATB (17, 18). The seminal transcriptomic signature of ATB prognosis was reported by Zak et al., comprising 16-genes specifically expressed in the blood of LTBI individuals prior progression to ATB, and associated with IFN signaling (19). More recently, we have identified a blood transcriptomic signature following anti-TB therapy shared between ATB patients and a subset of LTBI individuals, also enriched for IFN signaling genes (20).

Previous studies have shown differences in IgG glycosylation profiles between individuals with ATB and LTBI, including galactosylation of both total and *Mtb*-specific IgG (11, 12). Distinct IgG glycosylation profiles have also been reported in ATB before and after treatment (11). Among asymptomatic individuals, resisters (those with prolonged exposure to *Mtb* but no evidence for immunological memory or infection) show distinct glycosylation motifs in antigen-specific IgG compared to LTBI individuals (10, 13). Taken together, these findings suggest that IgG glycosylation may have utility in the clinical management of *Mtb* infection. However, no study has investigated these molecular features considering LTBI as a heterogeneous cohort, and specifically study LTBI individuals with a higher risk of developing ATB.

Here, we undertook extensive IgG glycosylation profiling in longitudinal samples from patients with ATB and LTBI before and after treatment, combined with matched full blood cell counts and transcriptomic signatures. Full blood counts and transcriptome were used to identify previously defined markers of risk of progression in ATB, and thus identify LTBI individuals with higher likelihood of progression to ATB (LTBI-Risk). Blood IgG glycosylation profiles were compared across cohorts and correlated with risk progression signatures.

Methods

Subjects and samples

Participants were enrolled at one of three clinical sites in Birmingham, Oxford or Catterick, UK. Enrollment of all participant groups was done simultaneously at the three clinical sites. ATB was defined as either a suspected (based on clinical suspicion and radiological and/or histological evidence) or microbiologically confirmed (by microscopy or *Mtb* culture) new diagnosis of pulmonary or extrapulmonary TB disease, in the absence of any other significant co-morbidity. LTBI status was confirmed in participants with a positive Interferon gamma release assays (IGRA; QuantiFERON-TB Gold In-Tube, Qiagen, Sunnyvale, California, or T-SPOT.TB, Oxford Immunotec) and the absence of clinical and radiographic signs of ATB or other significant co-morbidity. Uninfected control participants (TBneg cohort) were recruited as healthy controls at the same three clinical sites in whom ATB and LTBI were excluded and had no past medical history of ATB or evidence of previous exposure to *Mtb*, as confirmed by a negative IGRA test. All participants were HIV-negative adults (≥ 18 years). Anti-TB treatment was based on UK standard regimens of combination drug therapy (<https://www.nice.org.uk/guidance/cg117>). For the LTBI cohort, treatment was 3 months of daily rifampicin and isoniazid. For the ATB cohort, treatment consisted of 2 months of daily rifampicin, isoniazid, pyrazinamide, and ethambutol, followed by 4 months of daily rifampicin and isoniazid. All ATB participants had drug sensitive TB and successfully completed the 6 months treatment course, based on resolution of clinical symptoms and sputum conversion to negativity (where applicable). There was no occurrence of relapse or recurrence. Because all three clinical sites have a low *Mtb* incidence setting, it was presumed that the risk of re-infection was negligible for both LTBI and ATB participants. For the LTBI cohort, a post-treatment sample was obtained 4-10 months after the pre-treatment sample (corresponding to at least 1-7 months after completion of treatment). For the ATB cohort, a post-treatment sample were obtained 7-13 months after the pre-treatment sample (corresponding to at least 1-7 months after completion of treatment). For all samples, 2.5mL of blood was collected directly into a PAXgene® tube (BD Biosciences), mixed, and stored at -80°C until processing. An additional

6mL sample of clotted blood was collected from each participant and following centrifugation, serum was aliquoted and stored at -20°C .

Total IgG glycosylation profiling

Total IgG glycosylation profiling was performed blinded, where each sample was only associated with an arbitrary ID number, and the unblinding was performed at the analysis step. Total IgG was affinity-purified from 1 μl of serum using Protein G Sepharose Fast Flow beads (GE Healthcare, Uppsala, Sweden), followed by tryptic digestion to generate IgG Fc glycopeptides (21). Aliquots of tryptic digests were separated by liquid chromatography (LC) using the UltiMate™ 3000 RSLCnano System (Thermo Scientific) equipped with a PepMap 100 trap column and a nanoEase M/Z peptide column using a gradient from solvent-A (0.02% TFA in water) to 50% solvent-B (95% ACN) at 0.6 $\mu\text{l}/\text{min}$. The LC was coupled by electrospray ionization to a quadrupole time-of-flight mass spectrometer (Impact HD; Bruker Daltonics, Bremen, Germany) equipped with a nanoBooster. Ionization was enhanced by applying acetonitrile-doped nebulizing nitrogen gas at 0.2 bar. Profile spectra were recorded in an m/z range from 550 to 1800 with a frequency of 1 Hz. IgG Fc glycopeptides were identified on the basis of accurate mass and retention time. Relative quantification of IgG glycopeptide signals was performed using LaCyTools (22), and the glycosylation traits - galactosylation, sialylation, fucosylation and bisection - were calculated (23). A frozen pool of normal plasma from a minimum of 20 healthy controls (VisuConF, Affinity Biologicals) was used as a positive quality control for the assay. For all paired subjects (i.e., for which a sample was collected both prior to, and after completion of anti-TB treatment), changes over treatment were calculated by dividing pre-treatment values to post-treatment values for each IgG glycosylation trait (and referred to as post/pre-treatment).

Full blood count

Full blood count (FBC) was performed on whole blood in United Kingdom Accredited Service (UKAS)-accredited clinical laboratories using standard procedures. Each feature is expressed in its standard reference unit.

Whole blood transcriptomic analysis

Whole blood transcriptomic analysis was performed as previously described (20). Total intracellular RNA was extracted from PAXgene® samples using the Blood RNA Kit (Qiagen) according to the manufacturer's instructions. Globin mRNA was depleted from total RNA extractions using a biotin/streptavidin/magnetic bead-based assay, according to the manufacturer's instructions (GLOBINclear Kit, Ambion). The depleted RNA was then amplified and biotin-labeled using the TotalPrep RNA Amplification Kit (Illumina), followed by hybridization onto Illumina HumanHT-12 (v4.0) expression beadchips according to the manufacturer's instructions. Arrays were scanned with an Illumina bead array reader confocal scanner. The idat Illumina HumanHT12-V4 microarray files were converted to raw expression data using the Bioconductor package beadarray v2.38 (24) in R. The raw data was quantile normalized and log₂ transformed using the Bioconductor package lumi v2.40 (25) in R. A comprehensive annotation was performed using annotations provided by biomaRt v2.40.5, the Gene Expression Omnibus (GEO), and platform specific annotation obtained from Illumina. If there was not a consensus among annotations, biomaRt was given preference given its regular updates, followed by GEO, and lastly the platform specific annotation. For non-specific filtering median, coefficient of variation and inter-quartile range for all probes across all samples were calculated. The probes accounting for the bottom 50% in each measurement were overlapped, and those probes that fell in the bottom 50% of all measurements (n=20,147) were removed from further analysis, leaving a final set of 27,960 probes of the initial 48,107 probes. Batch effect was removed and normalization performed using the Combat function from the Bioconductor package sva v3.36 (26).

Bioinformatic analysis

Heatmaps and principal component analyses were constructed using raw IgG glycosylation prevalence values or combat normalized gene expression values with the bioinformatic software analysis Qlucore omics explorer, after centralized normalization (mean =0, standard deviation = 1 for each variable). All scores were calculated using standard z-score formulas. The antibody glycosylation score was calculated by subtracting IgG1-galactosylation values to IgG1-H3N4F1 values (glycan composition given in terms of hexose (H), N-acetylhexosamine (N) and fucose (F)). The fucosylation score was calculated by tallying IgG1 and IgG2/3 fucosylation values. The Zak16 gene signature score was calculated by tallying the normalized expression values for all probes mapping to one of the 16 genes included in the signature (19).

Gene Ontology Biological processes enrichment analysis was performed with the online platform enrichR (27). Expression of gene signatures in immune blood cell types were calculated with the CellTypeScore tool in DICE database (<http://dice-database.org/>). The DICE database contains gene expression data generated from 13 immune cell types (and 2 activation conditions) isolated from peripheral blood mononuclear cells of 91 healthy individuals (28). For a given gene list, the CellTypeScore tool sum the normalized expression values of each individual gene constituting the list for each of the cell types/stimulation conditions.

A K Nearest Neighbor (KNN) classifier analysis was performed using Qlucore omics explorer software and default parameters.

Statistics

All cross-sectional comparisons were performed using non-parametric unpaired Mann-Whitney tests. Statistical comparisons for individual glycosylation features or scores between cohorts were performed using Prism (version 9.4.1), using non-parametric Mann-Whitney tests, and considering $p < 0.05$ as significant. Linear regression and receiver operating characteristics (ROC) curve analyses were performed using Prism (version 9.4.1). Correlations were performed

using Spearman's rank correlation tests in Prism (version 9.4.1). Statistical significance of overlap between gene lists was calculated using the hypergeometric distribution test and considering all total genes present in the microarray dataset. Differentially expressed genes between High and Low score groups were identified using the two-comparison test statistic function from the bioinformatic software Qlucore omics explorer.

Ethics approval

Participants recruited for this study were enrolled under ethical approval granted by the National Research Ethics Service, Heart of England NHS Foundation Trust (2012107RM), Committee South Central - Oxford C (12/SC/0299) and the Ministry of Defence Research Ethics Committee (MoDREC 237/PPE/11), respectively. All samples were obtained for specific use in this study. All clinical investigations were conducted according to the principles of the Declaration of Helsinki, and all participants provided written informed consent prior to participation.

Results

Individuals with ATB and LTBI show distinct IgG glycosylation profiles prior to, but not after completion of anti-TB therapy

To investigate changes in antibody glycosylation in the context of *Mtb* infection and treatment, we measured the prevalence of 73 glycosylation features in total IgG from the sera of ATB patients and LTBI individuals collected prior to, and after completion of anti-TB therapy (n=19 ATB and n=56 LTBI pre-treatment; n=10 ATB and n= 42 LTBI post-treatment; including n=10 ATB and n=29 LTBI with paired pre- and post-treatment samples). Details regarding anti-TB therapy regimens, timeline and sample collection for both ATB and LTBI cohorts are available in the methods, subjects and samples section. A TBneg control group (n=23) was also included in the study, with only one time point collection. Demographics for all disease groups and treatment

cohorts are reported in **Table 1**. The relative abundance of all 73 IgG glycosylation features that were measured for each sample is available in **Table S1**, along with their proposed structure. Various combinations of 23 specific glycan structures (e.g., H3N4F1) were measured in IgG1, IgG2/3 and IgG4 subtypes. For each structure, the labelling refers to the glycan composition given in terms of hexoses (H), N-acetylhexosamines (N) and fucoses (F). In addition, total galactosylation, fucosylation, bisection, sialylation, and the ratio of sialylation/galactosylation were determined for IgG1, combined IgG2/3 and IgG4 subtypes. Unsupervised analysis of all features showed a clear separation between ATB and LTBI/TBneg cohorts prior to initiation of anti-TB therapy (**Figure 1A**), with many features downregulated in ATB (**Figure 1B**). In contrast, no distinction between cohorts was found in samples collected after anti-TB therapy (**Figure 1C** and **1D**). For paired samples, calculation of fold changes upon treatment (post/pre-treatment) for all features also revealed a complete segregation between ATB and LTBI cohorts (**Figure 1E**), with most features showing upregulation upon treatment (**Figure 1F**). There were no differences in IgG glycosylation profiles in ATB suspected vs confirmed cases (**Figure S1A-B**), and between paired (i.e., those with both pre- and post-treatment samples) vs unpaired (i.e., those with only one sampling timepoint) participants for both LTBI and ATB cohorts pre-treatment (**Figure S1C**) and post-treatment (**Figure S1D**). Whereas our dataset was not powered to systematically assess the impact of age, gender and race on IgG glycosylation profiles pre- and post-TB treatment, we nevertheless explored whether any of the above reported differences could be impacted by these demographic parameters. For the TBneg cohort, IgG glycosylation profiles were significantly different between male and female, and similarly between Asian and European (**Figure S2A-B**). These two observations were interlinked (all 5 female were also the only 5 participants of European race). No differences were found within LTBI or ATB cohorts split by gender or race (**Figure S2A-B**). Age was not significantly correlated with IgG glycosylation profiles in all 3 cohorts (**Figure S2C**). Thus, there was no obvious effect of age, gender or race in IgG glycosylation profiles within LTBI and ATB. In conclusion, individuals with ATB and LTBI show distinct IgG

glycosylation profiles prior to the initiation of anti-TB therapy, and these differences were not apparent anymore upon completion of treatment.

Two IgG1 glycosylation features can distinguish ATB from LTBI cohorts with high accuracy

Next, we aimed to reduce the dimensionality of the dataset and identify IgG glycosylation features that were responsible for the most differences between ATB and LTBI cohorts. We performed a KNN classifier analysis, to identify the minimum number of features necessary to achieve the highest accuracy of discrimination between ATB and LTBI cohorts using pre, post or post/pre-treatment values. The highest accuracy was achieved using post/pre-treatment values, and three features (Accuracy = 0.92) (**Figure 2A, B**). Pre-treatment values were associated with the second highest accuracy, using four features (Accuracy = 0.73), (**Figure 2A, B**). Post-treatment values were associated with the lowest accuracy of discrimination between ATB and LTBI (Accuracy = 0.59), and the highest number of features (n=17, Table S2). When included along the IgG glycosylation features, age was not selected as a significant variable by any of the classifiers. Two features were present in both pre and post/pre-treatment classifiers: IgG1-H3N4F1 (i.e., motif containing 4 N-acetylhexosamines, 3 mannoses, and 1 fucose, see proposed structure in Table S1) and IgG1-galactosylation (**Figure 2B**). The prevalence of the IgG1-H3N4F1 motif was significantly higher in ATB compared to LTBI and TBneg cohorts prior to treatment, and to a lesser degree post-treatment (**Figure 2C**); and its fold change upon treatment was significantly reduced in ATB compared to LTBI (**Figure 2C**). In contrast, the prevalence of IgG1-galactosylation was significantly lower in ATB compared to LTBI and TBneg cohorts prior to treatment, and to a lesser degree post-treatment (**Figure 2D**); and its fold change upon treatment was significantly increased in ATB compared to LTBI (**Figure 2D**). We combined these two features into one single metric by calculating an antibody glycosylation (AbGlyc) score, by subtracting the prevalence of IgG1-galactosylation (downregulated feature) to the prevalence of IgG1-H3N4F1 (upregulated feature) for each sample and time-point (pre, post, post/pre-treatment). The AbGlyc score was

significantly higher in ATB compared to LTBI and TBneg cohorts prior to treatment, and to a lesser degree post-treatment (**Figure 2E**); and its fold change post/pre-treatment was significantly higher in ATB compared to LTBI (**Figure 2E**). The AbGlyc score was highly efficient at distinguishing ATB from LTBI and ATB from TBneg cohorts prior to treatment (AUC = 0.90, $p < 0.0001$; and AUC = 0.92, $p < 0.0001$, respectively), but performed poorly for TBneg vs LTBI comparison (AUC of 0.61, $p = 0.15$) (**Figure 2F**). The accuracy of the AbGlyc score for distinguishing cohorts was also reduced post-treatment, with AUCs of 0.82, 0.80 and 0.55 (p values of 0.002, 0.006 and 0.55, respectively) for ATB vs LTBI, ATB vs TBneg and TBneg vs LTBI comparisons, respectively (**Figure 2G**). The highest accuracy of classification between ATB and LTBI was obtained with the AbGlyc score calculated with fold changes post/pre-treatment values, with a near perfect AUC of 0.99 ($p < 0.0001$, **Figure 2H**). The AbGlyc score was not correlated with age, nor associated with gender or race in the LTBI and ATB cohort (**Figure S3**). Thus, the combination of two bulk IgG1 glycosylation features, namely IgG1-H3N4F1 and IgG1-galactosylation, can discriminate ATB from LTBI with high accuracy. The highest accuracy was achieved using post/pre-treatment values, but a good efficacy (i.e., AUC >0.9) was also obtained solely using pre-treatment values.

The AbGlyc score correlates with blood cellular and transcriptomic signatures of ATB risk

Individuals with LTBI exist on a spectrum, ranging from recent exposure and high risk of progressing to ATB, as well as those that have resolved *Mtb* infection but have retained immune memory (14, 15). LTBI individuals at risk of developing ATB express a blood transcriptomic signature similar to those with ATB, and distinct from LTBI non-progressors (19). Assessing IgG glycosylation features using either unsupervised analysis (**Figure 1**), or individual features (**Figure 2**), we observed a large spread for the LTBI cohort, with some individuals holding values similar to ATB (**Figure 3**). We selected all LTBI samples which had both pre-treatment AbGlyc score and paired historic blood transcriptomic data available (20) ($n=56$). We sorted all LTBI pre-treatment samples based on their AbGlyc score, and identified the top 10 (AbGlyc score High)

and bottom 10 (AbGlyc score Low) individuals (**Figure 3A**). We then looked for transcriptomic differences between AbGlyc score High and Low groups. The top 100 differentially expressed genes (corresponding to a p value < 0.005) contained a majority of genes upregulated in the AbGlyc score High group (81 genes, **Figure 3B**). These 81 genes were significantly enriched for genes associated with type I and type II IFN signaling (**Figure 3C**). Additionally, this gene signature significantly overlapped with the previously published 16-gene IFN-risk signature expressed by LTBI progressors (also referred to as Zak16 (19)) with 5 genes in common (**Figure 3D**), and the AbGlyc score positively correlated with the Zak16 gene signature score (**Figure 3E**). Another prospective marker of risk of progression to ATB is the monocyte to lymphocyte ratio (M/L ratio) in blood (17, 18). The AbGlyc score was positively correlated with the M/L ratio (**Figure 3F**), and to a lesser extent with monocyte, neutrophil and platelet counts (**Figure S4**). Thus, the two IgG glycosylation features with the highest classification accuracy to distinguish ATB from LTBI and TBNeg were also positively associated with previously published markers of risk of progression to ATB.

The pre-treatment AbGlyc score is highly expressed in LTBI-Risk individuals

We have recently reported the distinction between LTBI-Risk and LTBI-Other individuals based on the expression of the IFN-risk (or Zak16) gene signature (19) prior to treatment (20). We showed that LTBI-Risk individuals (i.e., LTBI individuals with high expression of the Zak16 signature pre-treatment) have blood transcriptomic changes after treatment distinct from the LTBI cohort at large (i.e., LTBI-Other), and similar to ATB, suggesting a subclinical TB disease phenotype (20). Thus, we investigated whether the AbGlyc score could distinguish between LTBI-Risk and LTBI-Other individuals. The AbGlyc score was significantly upregulated in LTBI-Risk compared to LTBI-Other or TBNeg cohorts, and further upregulated in ATB compared to LTBI-Risk, LTBI-Other and TBNeg cohorts (**Figure 3G**). Using the AbGlyc score on this new classification, LTBI-Risk individuals were significantly distinguishable from all three cohorts (AUC

= 0.82, $p = 0.005$; AUC 0.71, $p = 0.036$; and AUC = 0.73, $p = 0.038$ for ATB, LTBI-Other and TBneg comparisons against LTBI-Risk, respectively) (**Figure 3H**). Thus, the AbGlyc score could not only distinguish ATB from LTBI, but also within LTBI individuals, identify those who may be at higher risk of progressing to ATB.

Pre-treatment IgG fucosylation levels are elevated in LTBI-Risk individuals and associate with NK-cell gene signatures

Next, we investigated whether additional IgG glycosylation features could specifically distinguish LTBI-Risk individuals from the remaining LTBI cohort. When revisiting the unsupervised PCA analysis presented in **Figure 1A**, but this time dividing the LTBI cohort into LTBI-Risk and LTBI-Other individuals, we observed that whereas PC1 was clearly associated with ATB, PC2 was associated with LTBI-Risk, with all LTBI-Risk individuals presenting negative PC2 values (**Figure 4A**). Of the top 10 variables associated with PC2, the highest two were fucosylation traits (IgG1 and IgG2/3 fucosylation), and were negatively weighting with the PC2 value (and thus expected to be at higher prevalence in LTBI-Risk group compared to other cohorts) (**Figure 4B**). Both features showed a significantly higher prevalence in LTBI-Risk compared to LTBI-Other cohorts, and IgG1 fucosylation was additionally significantly higher in LTBI-Risk compared to the TBneg cohort (**Figure 4C**). Interestingly, the prevalence of IgG4 fucosylation was unchanged across cohorts (**Figure S5**). Similar to the AbGlyc score, we calculated a fucosylation score, by tallying the relative abundance values for IgG1 and IgG2/3 fucosylation for each sample. The fucosylation score was significantly higher in LTBI-Risk compared to LTBI-Other and TBneg cohorts, and slightly higher in LTBI-Risk compared to ATB individuals, but not significantly (**Figure 4D**). In order to define transcriptomic signatures associated with fucosylation in LTBI, we sorted all LTBI pre-treatment samples based on their fucosylation score, and identified the top 10 (fucosylation score High) and the bottom 10 (fucosylation score Low) individuals (**Figure 4E**). We then looked for transcriptomic differences between fucosylation score High and Low groups. Almost half of

the top 200 differentially expressed genes (corresponding to a p value < 0.016) were upregulated in the fucosylation High group (n=95, 47%), compared to the fucosylation Low group (n=105, 53%) (**Figure 4F**). None of the upregulated or downregulated genes in the fucosylation High group showed significant enrichment for GO biological processes. Downregulated genes in the fucosylation High group were strongly associated with NK cells, including genes highly specific to cytotoxicity (e.g. PRF1 and NKG7) (**Figure 4G**). In contrast, genes upregulated in the fucosylation High group were similarly expressed across immune cell types (**Figure 4H**). Thus, fucosylation on IgG1 and IgG2/3 is elevated in LTBI-Risk individuals and negatively correlates with transcriptomic signatures associated with NK cells.

Discussion

In this study, we undertook comprehensive glycosylation profiling of total IgG in individuals with ATB and LTBI before and after anti-TB treatment, in combination with matched blood cellular and transcriptomic signatures. We found that glycosylation features on total IgG varied greatly between ATB compared to LTBI and uninfected controls, and also upon treatment. After treatment, the IgG glycosylation profile in ATB was more similar to the control cohorts. Dimensionality reduction analysis identified that the prevalence of two bulk IgG1 glycosylation features, namely IgG1-H3N4F1 and IgG1-galactosylation, could distinguish ATB from the other two cohorts with high accuracy when assessing changes upon treatment, but also using pre-treatment samples only. The H3N4F1 motif was at increased prevalence, whereas galactostylation was reduced in IgG1 from individuals with ATB.

IgG1 is the most common Ig circulating in blood, and is the most well-characterized and understood subclass of IgG, especially in the context of infection (29). Antigen-specific IgG1 against a variety of *Mtb* antigens have been shown to be at elevated levels in ATB, and to a lower

extent in LTBI (30, 31). Reduced levels of galactosylation on total IgG is commonly found in acute inflammation and with ageing (4-6), whereas pregnancy has the opposite effect (32). In *Mtb*, digalactosylated total IgG were at lower prevalence in ATB compared to LTBI, and compared to treated ATB (11, 12), consistent with results presented here. Increased galactosylation enhances IgG1-mediated complement activation (33). Thus, the reduction in galactosylation motifs in IgG1 in ATB may be a hallmark of uncontained infection, possibly due to lower complement activation.

Our finding that only two bulk IgG1 features were sufficient to distinguish between ATB and LTBI prior treatment with high accuracy (AUC = 0.90, $p < 0.0001$, Figure 2F) was striking. The fact that such a discriminatory power was obtained using pre-treatment samples hold significant potential for improving the molecular diagnosis for ATB. According to WHO's guidelines, formal diagnosis of ATB should be achieved using a sputum sample, with either detection of *Mtb* nucleic acid or bacilli directly *ex vivo* or after *in vitro* culture. This method is fastidious, and some individuals remain sputum negative, while displaying radiographic and clinical symptoms consistent with ATB. An IgG glycosylation plasma-based assay could have utility as an additional diagnostic tool in such individuals and holds greater logistical advantages, as blood is safer and easier to access than sputum, and the measurement of IgG glycosylation features is a robust and standardizable assay. The assay may also even work on saliva, as glycosignatures of bulk IgG from blood and saliva are highly similar (34). Furthermore, such a test may be able to detect ATB cases that are both sputum positive and negative. Indeed, as shown in Figure S1, both confirmed and suspicious cases of ATB showed similar glycosylation profiles, distinct from LTBI and uninfected controls.

More importantly, the two total IgG1 glycosylation features correlated with the expression of IFN-associated genes and M/L ratio (two prospective blood markers of ATB), and could identify within LTBI, individuals with a blood transcriptomic signature associated with a higher risk of progression to ATB (LTBI-Risk). Interrupting TB transmission by prompt diagnosis and treatment of ATB is

key to reducing disease prevalence and mortality. However, managing individuals with LTBI is also needed to achieve the WHO's TB elimination goals (35, 36). A significant limitation to this is the current inability to identify LTBI individuals at high risk of progressing to ATB. The historic binary classification of patients as either asymptomatic LTBI or symptomatic ATB does not capture the full heterogeneity and overlap between TB infection states. There is increasing recognition that LTBI is a spectrum, ranging from those who have eliminated the pathogen to individuals with subclinical active disease (37-39). The control of TB requires understanding the full spectrum of infection to allow the development of new diagnostic approaches for identifying individuals with LTBI at risk of ATB and who would most benefit from preventative treatment (40). Recent work has shown that resisters (individuals with prolonged exposure to *Mtb* but no evidence for immunological memory or infection) have a different IgG glycosylation profile compared to LTBI (10, 13). Here, we identified that IgG glycosylation features such as IgG1-H3N4F1 and IgG1-galactosylation may be valuable biomarkers to further characterize the TB spectrum, by monitoring the risk of ATB disease progression in the LTBI pool.

Additional changes specific to the LTBI-Risk group included increased prevalence of fucosylation on IgG1, IgG2/3, but not IgG4. The degree of fucosylation on IgG Fc regulates effector functions of humoral immunity, by impacting the antibody's ability to interact with Fc gamma receptors (41). Circulating IgG are typically highly fucosylated, while afucosylated antigen-specific IgG are produced against pathogens whose antigens are localized on the host cell membrane, such as enveloped viruses (e.g., HIV, Sars-cov2 (42)) or intracellular pathogens (e.g., *Plasmodium falciparum* (43)). In *Mtb* infection, high levels of fucosylation on total IgG have been reported in ATB compared to LTBI (44). Thus, IgG fucosylation may be an additional functional biomarker to identify within LTBI, those at risk of progression to ATB.

A high fucosylation prevalence prior to treatment was associated with transcriptomic changes related to NK cells (negative correlation). The frequency of NK cells is decreased in ATB compared to LTBI, and during progression from LTBI to ATB (45), and we have shown downregulation of NK cell genes upon treatment in ATB (20). In addition, IgG in LTBI have superior NK-mediated cytotoxicity compared to ATB, likely mediated by distinct glycosylation features such as lower levels of fucosylation (44). Collectively, these previous studies and our observations suggest that NK cells, which have a significant protective role against *Mtb*, may play a direct or indirect role in the regulation of IgG glycosylation processes, in particular fucosylation.

There were limitations associated with our study design. First, this was an exploratory study and to determine whether IgG glycosylation traits could be used as test for TB diagnosis or prognosis, validation in a larger and more diverse cohort (i.e., geographic location, *Mtb* prevalence, immunodeficiency status, etc.) is necessary. Second, to identify whether our newly identified IgG glycosylation signature is specific to *Mtb*, or simply indicative of an active respiratory disease, the ATB cohort should be compared to a no TB disease group (such as patients with bacterial pneumonia, non-tuberculous mycobacteria, or granulomatous lung diseases such as sarcoidosis). Third, our small sample size in the ATB group precluded investigating the association between treatment success and IgG glycosylation. The striking difference in IgG glycosylation profiles between pre- and post-treatment visits in ATB suggest that treatment failures may be associated with a distinct IgG glycosylation profile post-treatment compared to successful treatment, with failures resembling ATB prior to treatment. Additional sampling closer to the start of treatment will help determine when changes in IgG glycosylation mostly occur, and may allow for prediction of treatment failure. Fourth, our analysis focused on total IgG features, rather than antigen-specific IgG. Whether *Mtb*-specific IgG show similar glycosylation differences across TB cohorts remains to be determined.

There is currently no single biomarker that can predict progression from LTBI to ATB with high accuracy across studies, and using a combination of parameters may be a superior approach. While large prospective studies in both high and low endemic settings are needed, our findings provide the first evidence that measurement of glycosylation features of total IgG1 could be used in combination with already available blood cellular and RNA biomarkers to identify individuals with LTBI at risk of progression to ATB. We suggest that future studies of LTBI prognosis include the measurement of IgG glycosylation features.

Funding

This work was supported by The University of Birmingham.

Acknowledgments

The authors thank Jan Nouta for his assistance with IgG Fc glycosylation analysis.

Contributors

MKO, MW and AFC designed the research study. WW and MW conducted experiments. JGB analyzed data. MD, TEF and MKO obtained clinical samples. JGB and MKO wrote the manuscript, with input from all other co-authors.

Declaration of interests

The authors have declared that no conflict of interest exists.

Data sharing statement

The complete IgG glycosylation data is available in Table S1. Microarray data has been deposited to NCBI's Gene Expression Omnibus (GEO) database repository and is available under GEO accession number GSE152532.

References

1. Jefferis R. Glycosylation as a strategy to improve antibody-based therapeutics. *Nat Rev Drug Discov.* 2009;8(3):226-34.

2. Arnold JN, Wormald MR, Sim RB, Rudd PM, Dwek RA. The impact of glycosylation on the biological function and structure of human immunoglobulins. *Annu Rev Immunol.* 2007;25:21-50.
3. Lu LL, Suscovich TJ, Fortune SM, Alter G. Beyond binding: antibody effector functions in infectious diseases. *Nat Rev Immunol.* 2018;18(1):46-61.
4. Parekh R, Roitt I, Isenberg D, Dwek R, Rademacher T. Age-related galactosylation of the N-linked oligosaccharides of human serum IgG. *J Exp Med.* 1988;167(5):1731-6.
5. Seeling M, Bruckner C, Nimmerjahn F. Differential antibody glycosylation in autoimmunity: sweet biomarker or modulator of disease activity? *Nat Rev Rheumatol.* 2017;13(10):621-30.
6. Plomp R, Ruhaak LR, Uh HW, Reiding KR, Selman M, Houwing-Duistermaat JJ, et al. Subclass-specific IgG glycosylation is associated with markers of inflammation and metabolic health. *Sci Rep.* 2017;7(1):12325.
7. Ferrara C, Grau S, Jager C, Sondermann P, Bruncker P, Waldhauer I, et al. Unique carbohydrate-carbohydrate interactions are required for high affinity binding between FcγRIII and antibodies lacking core fucose. *Proc Natl Acad Sci U S A.* 2011;108(31):12669-74.
8. de Jong SE, Selman MH, Adegnikaa AA, Amoah AS, van Riet E, Kruize YC, et al. IgG1 Fc N-glycan galactosylation as a biomarker for immune activation. *Sci Rep.* 2016;6:28207.
9. Selman MH, de Jong SE, Soonawala D, Kroon FP, Adegnikaa AA, Deelder AM, et al. Changes in antigen-specific IgG1 Fc N-glycosylation upon influenza and tetanus vaccination. *Mol Cell Proteomics.* 2012;11(4):M111 014563.
10. Davies LRL, Smith MT, Cizmeci D, Fischinger S, Shih-Lu Lee J, Lu LL, et al. IFN-γ independent markers of Mycobacterium tuberculosis exposure among male South African gold miners. *EBioMedicine.* 2023;93:104678.
11. Grace PS, Dolatshahi S, Lu LL, Cain A, Palmieri F, Petrone L, et al. Antibody Subclass and Glycosylation Shift Following Effective TB Treatment. *Front Immunol.* 2021;12:679973.
12. Lu LL, Das J, Grace PS, Fortune SM, Restrepo BI, Alter G. Antibody Fc Glycosylation Discriminates Between Latent and Active Tuberculosis. *J Infect Dis.* 2020;222(12):2093-102.
13. Lu LL, Smith MT, Yu KKQ, Luedemann C, Suscovich TJ, Grace PS, et al. IFN-γ-independent immune markers of Mycobacterium tuberculosis exposure. *Nat Med.* 2019;25(6):977-87.
14. Behr MA, Kaufmann E, Duffin J, Edelstein PH, Ramakrishnan L. Latent Tuberculosis: Two Centuries of Confusion. *Am J Respir Crit Care Med.* 2021;204(2):142-8.
15. Pai M, Behr MA, Dowdy D, Dheda K, Divangahi M, Boehme CC, et al. Tuberculosis. *Nat Rev Dis Primers.* 2016;2:16076.
16. Shea KM, Kammerer JS, Winston CA, Navin TR, Horsburgh CR, Jr. Estimated rate of reactivation of latent tuberculosis infection in the United States, overall and by population subgroup. *Am J Epidemiol.* 2014;179(2):216-25.
17. Naranbhai V, Hill AV, Abdool Karim SS, Naidoo K, Abdool Karim Q, Warimwe GM, et al. Ratio of monocytes to lymphocytes in peripheral blood identifies adults at risk of incident tuberculosis among HIV-infected adults initiating antiretroviral therapy. *J Infect Dis.* 2014;209(4):500-9.

18. Naranbhai V, Kim S, Fletcher H, Cotton MF, Violari A, Mitchell C, et al. The association between the ratio of monocytes:lymphocytes at age 3 months and risk of tuberculosis (TB) in the first two years of life. *BMC Med.* 2014;12:120.
19. Zak DE, Penn-Nicholson A, Scriba TJ, Thompson E, Suliman S, Amon LM, et al. A blood RNA signature for tuberculosis disease risk: a prospective cohort study. *Lancet.* 2016;387(10035):2312-22.
20. Burel JG, Singhanian A, Dubelko P, Muller J, Tanner R, Parizotto E, et al. Distinct blood transcriptomic signature of treatment in latent tuberculosis infected individuals at risk of developing active disease. *Tuberculosis (Edinb).* 2021;131:102127.
21. Pongracz T, Nouta J, Wang W, van Meijgaarden KE, Linty F, Vidarsson G, et al. Immunoglobulin G1 Fc glycosylation as an early hallmark of severe COVID-19. *EBioMedicine.* 2022;78:103957.
22. Jansen BC, Falck D, de Haan N, Hipgrave Ederveen AL, Razdorov G, Lauc G, et al. LaCyTools: A Targeted Liquid Chromatography-Mass Spectrometry Data Processing Package for Relative Quantitation of Glycopeptides. *J Proteome Res.* 2016;15(7):2198-210.
23. Falck D, Jansen BC, de Haan N, Wuhler M. High-Throughput Analysis of IgG Fc Glycopeptides by LC-MS. *Methods Mol Biol.* 2017;1503:31-47.
24. Dunning MJ, Smith ML, Ritchie ME, Tavare S. beadarray: R classes and methods for Illumina bead-based data. *Bioinformatics.* 2007;23(16):2183-4.
25. Du P, Kibbe WA, Lin SM. lumi: a pipeline for processing Illumina microarray. *Bioinformatics.* 2008;24(13):1547-8.
26. Leek JT, Johnson WE, Parker HS, Jaffe AE, Storey JD. The sva package for removing batch effects and other unwanted variation in high-throughput experiments. *Bioinformatics.* 2012;28(6):882-3.
27. Chen EY, Tan CM, Kou Y, Duan Q, Wang Z, Meirelles GV, et al. Enrichr: interactive and collaborative HTML5 gene list enrichment analysis tool. *BMC Bioinformatics.* 2013;14:128.
28. Schmiedel BJ, Singh D, Madrigal A, Valdovino-Gonzalez AG, White BM, Zapardiel-Gonzalo J, et al. Impact of Genetic Polymorphisms on Human Immune Cell Gene Expression. *Cell.* 2018;175(6):1701-15 e16.
29. Vidarsson G, Dekkers G, Rispens T. IgG subclasses and allotypes: from structure to effector functions. *Front Immunol.* 2014;5:520.
30. Mattos AM, Chaves AS, Franken KL, Figueiredo BB, Ferreira AP, Ottenhoff TH, et al. Detection of IgG1 antibodies against Mycobacterium tuberculosis DosR and Rpf antigens in tuberculosis patients before and after chemotherapy. *Tuberculosis (Edinb).* 2016;96:65-70.
31. de Araujo LS, da Silva NBM, Leung JAM, Mello FCQ, Saad MHF. IgG subclasses' response to a set of mycobacterial antigens in different stages of Mycobacterium tuberculosis infection. *Tuberculosis (Edinb).* 2018;108:70-6.
32. van de Geijn FE, Wuhler M, Selman MH, Willemsen SP, de Man YA, Deelder AM, et al. Immunoglobulin G galactosylation and sialylation are associated with pregnancy-induced improvement of rheumatoid arthritis and the postpartum flare: results from a large prospective cohort study. *Arthritis Res Ther.* 2009;11(6):R193.
33. Nimmerjahn F, Vidarsson G, Cragg MS. Effect of posttranslational modifications and subclass on IgG activity: from immunity to immunotherapy. *Nat Immunol.* 2023.

34. Plomp R, de Haan N, Bondt A, Murli J, Dotz V, Wuhrer M. Comparative Glycomics of Immunoglobulin A and G From Saliva and Plasma Reveals Biomarker Potential. *Front Immunol.* 2018;9:2436.
35. Abu-Raddad LJ, Sabatelli L, Achterberg JT, Sugimoto JD, Longini IM, Jr., Dye C, et al. Epidemiological benefits of more-effective tuberculosis vaccines, drugs, and diagnostics. *Proc Natl Acad Sci U S A.* 2009;106(33):13980-5.
36. Dye C, Glaziou P, Floyd K, Raviglione M. Prospects for tuberculosis elimination. *Annu Rev Public Health.* 2013;34:271-86.
37. Barry CE, 3rd, Boshoff HI, Dartois V, Dick T, Ehrt S, Flynn J, et al. The spectrum of latent tuberculosis: rethinking the biology and intervention strategies. *Nat Rev Microbiol.* 2009;7(12):845-55.
38. Drain PK, Bajema KL, Dowdy D, Dheda K, Naidoo K, Schumacher SG, et al. Incipient and Subclinical Tuberculosis: a Clinical Review of Early Stages and Progression of Infection. *Clin Microbiol Rev.* 2018;31(4).
39. Behr MA, Edelstein PH, Ramakrishnan L. Revisiting the timetable of tuberculosis. *BMJ.* 2018;362:k2738.
40. Esmail H, Macpherson L, Coussens AK, Houben R. Mind the gap - Managing tuberculosis across the disease spectrum. *EBioMedicine.* 2022;78:103928.
41. Oosterhoff JJ, Larsen MD, van der Schoot CE, Vidarsson G. Afucosylated IgG responses in humans - structural clues to the regulation of humoral immunity. *Trends Immunol.* 2022;43(10):800-14.
42. Larsen MD, de Graaf EL, Sonneveld ME, Plomp HR, Nouta J, Hoepel W, et al. Afucosylated IgG characterizes enveloped viral responses and correlates with COVID-19 severity. *Science.* 2021;371(6532).
43. Larsen MD, Lopez-Perez M, Dickson EK, Ampomah P, Tuikue Ndam N, Nouta J, et al. Afucosylated Plasmodium falciparum-specific IgG is induced by infection but not by subunit vaccination. *Nat Commun.* 2021;12(1):5838.
44. Lu LL, Chung AW, Rosebrock TR, Ghebremichael M, Yu WH, Grace PS, et al. A Functional Role for Antibodies in Tuberculosis. *Cell.* 2016;167(2):433-43 e14.
45. Roy Chowdhury R, Vallania F, Yang Q, Lopez Angel CJ, Darboe F, Penn-Nicholson A, et al. A multi-cohort study of the immune factors associated with M. tuberculosis infection outcomes. *Nature.* 2018;560(7720):644-8.

Table

Table 1: Cohorts composition and demographics.

Disease group	Treatment cohort	N	Age		Gender	Race			
			Range	Mean		% F/ %M	% EU	% AFR	% AS

LTBI	Pre	56	[18-56]	29	46/54	13	30	53	4
	Post	42	[18-40]	25	31/69	7	20	71	2
	Paired Pre/Post	29	[18-40]	27	45/55	11	29	57	4
ATB	Pre	19	[18-60]	33 [#]	21/79	11	22	67	0
	Paired Pre/Post	10	[18-60]	33 [§]	20/80	10	20	70	0
TBneg	-	15 [*]	[18-46]	25	33/67	33	0	67	0

*Demographics available for 15/23 control subjects

[#]Significantly older than TBneg ($p = 0.029$)

[§]Significantly older than LTBI-Post ($p = 0.026$)

F: Female; M: Male; EU: European; AFR: African; AS: Asian

Figure legends

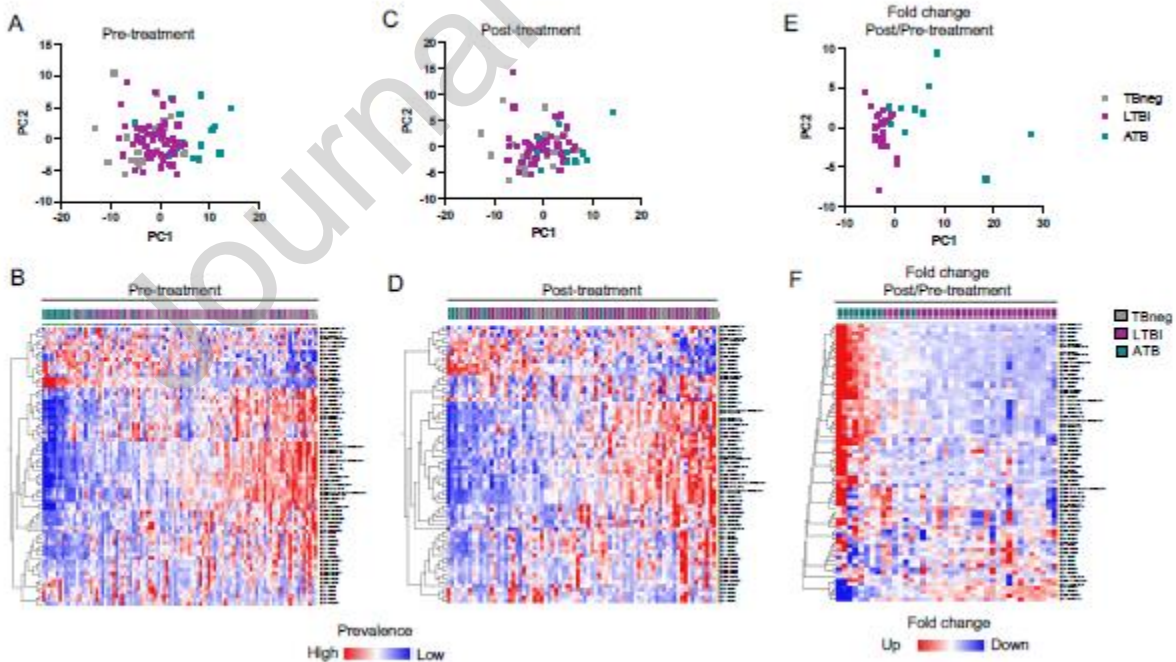


Figure 1: ATB and LTBI hold distinct IgG glycosylation profiles prior to, but not after completion of anti-TB therapy. Relative abundance of 73 distinct IgG glycosylation features pre-treatment (A,B), post-treatment (C,D) and post/pre-treatment (E,F) in ATB, LTBI and TBneg individuals, using PCA analysis (A,C,E) or heatmap representation (B,D,F). For the heatmap representation, individuals were sorted by decreasing PC1, and variables by hierarchical clustering. Data was derived from 19 ATB pre-treatment, 10 ATB post-treatment and 10 ATB paired post/pre-treatment samples; 56 LTBI pre-treatment, 42 LTBI post-treatment and 29 paired post/pre-treatment samples; and 23 TBneg samples.

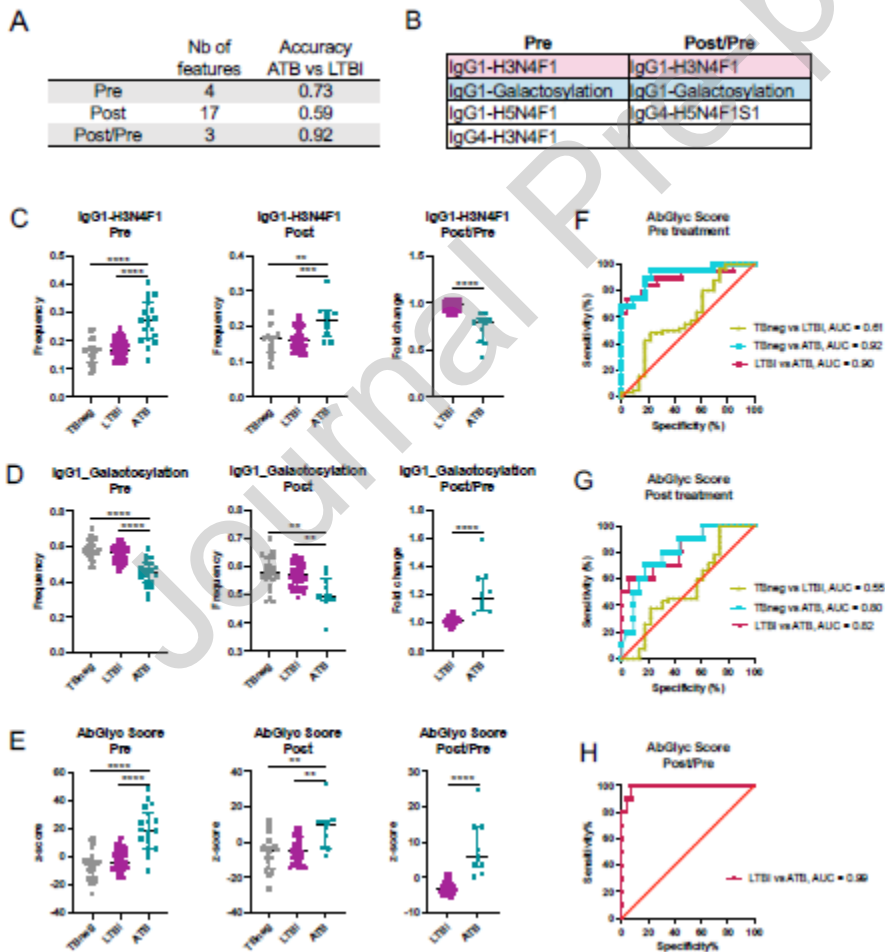


Figure 2: Two IgG1 glycosylation features are sufficient to distinguish ATB from LTBI and TBneg controls cohorts with high accuracy. A) Summary of results and B) individual features from the KNN classifier analysis to identify the minimum number of IgG glycosylation features with the highest classification accuracy across ATB, LTBI and TBneg cohorts using pre-treatment, post-treatment or post/pre-treatment values. C) Prevalence of H3N4F1 motif on total IgG1 pre-treatment, post-treatment and post/pre-treatment in ATB, LTBI and TBneg cohorts. D) Prevalence of galactosylation on total IgG1 pre-treatment, post-treatment and post/pre-treatment in ATB, LTBI and TBneg cohorts. E) Antibody glycosylation (AbGlyc) score pre-treatment, post-treatment and post/pre-treatment in ATB, LTBI and TBneg cohorts. The AbGlyc score was calculated by subtracting IgG1-galactosylation prevalence values to IgG1-H3H4F1 values and using a z-score standard formula. Receiver operating characteristic (ROC) curves quantifying the ability of the AbGlyc score to distinguish pairwise comparisons between ATB, LTBI and TBneg cohorts pre-treatment (F), post-treatment (G), and post/pre-treatment (H). Data was derived from 19 ATB pre-treatment, 10 ATB post-treatment and 10 ATB paired post/pre-treatment samples; 56 LTBI pre-treatment, 42 LTBI post-treatment and 29 paired post/pre-treatment samples; and 23 TBneg samples. ** $p < 0.01$; *** $p < 0.001$; **** $p < 0.0001$.

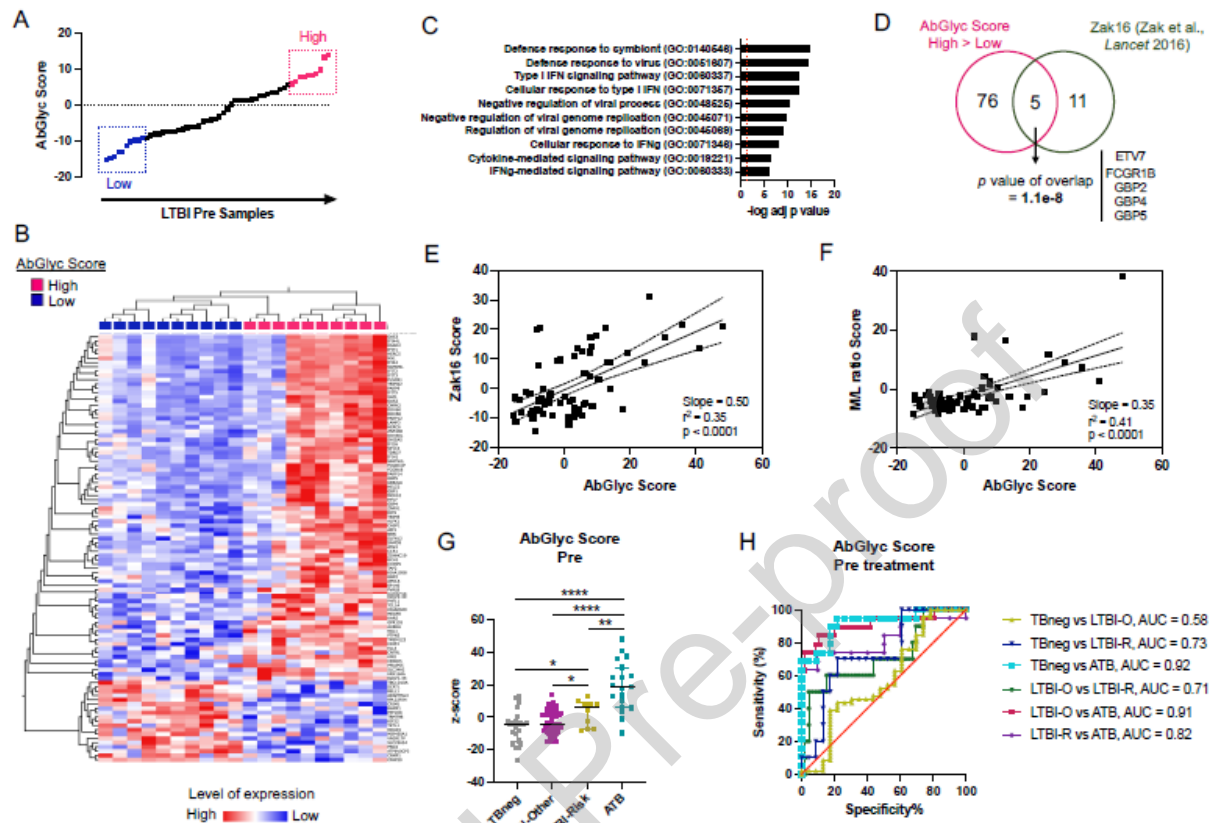


Figure 3: IgG1 glycosylation features at higher prevalence in ATB are also associated with molecular markers of progression to ATB in LTBI. A) Identification of the top 10 (High) and bottom 10 (Low) LTBI individuals ranked based on their antibody glycosylation (AbGlyc) score pre-treatment. The AbGlyc score was calculated by subtracting IgG1-galactosylation prevalence values to IgG1-H3H4F1 values and using a z-score standard formula. B) Top 100 genes differentially expressed pre-treatment between AbGlyc score High and Low groups defined by whole blood microarray analysis. C) Gene Ontology (GO) Biological processes enrichment analysis in the upregulated genes in the AbGlyc score High group (as shown in B). The downregulated genes showed no significant enrichment for GO Biological processes. D) Overlap between upregulated genes in the AbGlyc score High group (as shown in B) and the Zak16 gene signature (19). Linear regression (solid line) and 95% confidence intervals of the regression

(dotted lines) between the AbGlyc score and E) the Zak16 score, and F) the M/L ratio. All values were derived from pre-treatment samples. G) The AbGlyc score pre-treatment in ATB, LTBI-Risk, LTBI-Other and TBneg cohorts. Division of the LTBI cohort into LTBI-Risk and LTBI-Other group was based on the expression of the Zak16 signature in whole blood pre-treatment, as defined in (20). H) Receiver operating characteristic (ROC) curves quantifying the ability of the AbGlyc score pre-treatment to distinguish pairwise comparisons between ATB, LTBI-Risk (LTBI-R), LTBI-Other (LTBI-O), and TBneg cohorts. Data was derived from 19 ATB, 56 LTBI, and 23 TBneg samples. * $p < 0.05$; ** $p < 0.01$; **** $p < 0.0001$.

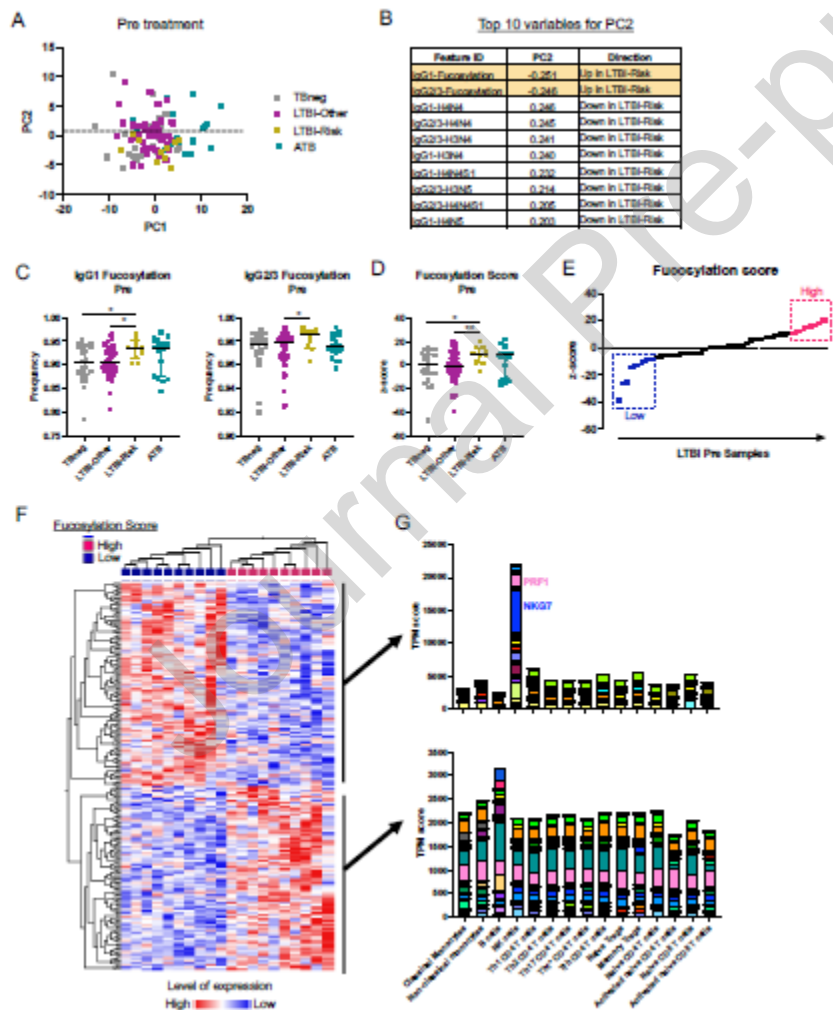


Figure 4: Increased prevalence of IgG fucosylation in LTBI-Risk individuals associates with NK-cell and B-cell gene signatures. A) PCA analysis of all 73 IgG glycosylation features pre-

treatment in ATB, LTBI-Risk, LTBI-Other and TBneg cohorts. Division of the LTBI cohort into LTBI-Risk and LTBI-Other group was based on the expression of the Zak16 signature (19) in whole blood pre-treatment, as defined in (20). B) Top 10 variables weighting for PC2, ranked by decreasing absolute value. The top two features were negatively weighted and highlighted in yellow. C) Prevalence of fucosylation on IgG1 (left panel) and IgG2/3 (right panel) pre-treatment in ATB, LTBI-Risk, LTBI-Other and TBneg cohorts. D) Fucosylation score pre-treatment in ATB, LTBI-Risk, LTBI-Other and TBneg cohorts. The fucosylation score was calculated by tallying IgG1 and IgG2/3 fucosylation prevalence values and using a z-score standard formula. E) Identification of the top 10 (High) and bottom 10 (Low) LTBI individuals ranked based on their fucosylation score pre-treatment. F) Top 200 genes differentially expressed pre-treatment between fucosylation score High and Low groups defined by whole blood microarray analysis. G) Immune cell type-specific expression of the G) top downregulated genes, and H) top downregulated genes in the fucosylation High group. Each bar consists of stacked sub-bars showing the TPM normalized expression of every gene in corresponding cell type, extracted from the DICE database (28) (<http://dice-database.org/>). Data was derived from 19 ATB, 56 LTBI, and 23 TBneg samples. * $p < 0.05$; ** $p < 0.01$

Declaration of Competing Interest

none

Research Highlights

- Serum antibody glycosylation profile is greatly disrupted in tuberculosis
- Two antibody glycosylation traits distinguished active from latent tuberculosis
- Several traits correlated with biomarkers of active tuberculosis risk
- Serum antibody glycosylation may be used as a biomarker to monitor tuberculosis